EUROPEAN COOPERATION
IN THE FIELD OF SCIENTIFIC
AND TECHNICAL RESEARCH

EURO-COST

SOURCE: Graz University of Technology, Austria

CA15104 TD(16)02018
Durham, England
October 4th-6th, 2016

MIMO Gain and Bandwidth Scaling for RFID Positioning in Dense Multipath Channels

Stefan Hinteregger, Erik Leitinger, Paul Meissner, Klaus Witrisal
Address for Stefan Hinteregger:
Graz University of Technology
Inffeldgasse 16c
A-8010 Graz
Austria
Phone: +43 316 873 4368
Fax: +43 316 873 104368

Email: stefan.hinteregger@tugraz.at, erik.leitinger@tugraz.at, paul.meissner@tugraz.at, witrisal@tugraz.at

MIMO Gain and Bandwidth Scaling for RFID Positioning in Dense Multipath Channels

Stefan Hinteregger, Erik Leitinger, Paul Meissner, Klaus Witrisal
Graz University of Technology, Austria; email: stefan.hinteregger@tugraz.at

***Abstract*—This paper analyzes the achievable ranging and positioning performance for two design constraints in a radio frequency identification (RFID) system: (*i*) the bandwidth of the transmit signal and (*ii*) the use of multiple antennas at the readers. The ranging performance is developed for correlated and uncorrelated constituent channels by utilizing a geometry-based stochastic channel model for the downlink and the uplink. The ranging error bound is utilized to compute the precision gain for a ranging scenario with multiple collocated transmit and receive antennas. The position error bound is then split into a monostatic and bistatic component to analyze the positioning performance in a multiple input, multiple output (MIMO) RFID system. Simulation results indicate that the ranging variance is approximately halved when utilizing uncorrelated constituent channels in a monostatic setup. It is shown that both the bandwidth and the number of antennas decrease the error variance roughly quadratically.**

***Index Terms*—Cramér-Rao bound, dense multipath channels, RFID, ranging, positioning, indoor environments, diversity, MIMO.**

I. Introduction

RFID tags have penetrated every corner of our lifes, but are paramount in supply chain management and logistics. One major detriment of passive RFID technology is its unsatisfying localization capability. In numerous applications like sorting of goods, intelligent warehouses, flexible production, etc., a sub-meter or even sub-decimetre positioning would be needed.

A trend towards signals with higher bandwidth has been established, for both active and passive RFID tags, to achieve higher accuracy for localization purposes [2]. Dardari and coworkers have focused on ultrawide-bandwidth (UWB) tags with the capability to scatter back a spreading sequence for CDMA [3], while others have only adapted the readers and used existing tags for radar like scenarios (e.g. [4]).

Several researchers have analyzed performance bounds for ranging and positioning with ultra-wideband (UWB) radio signals [5], [6]. In UWB settings, the channel is often modeled as a combination of specular reflections and so-called dense or diffuse multipath (DM) which comprises all other "energy producing" components [7] that cannot be resolved by the measurement aperture. By decreasing the bandwidth and thus going from UWB to conventional wideband radio signals the specular reflections cannot be isolated from the line-of-sight (LOS) component anymore, leading to a pulse distortion and fading effect. In [8] we analysed the ranging and positioning error bound for these conventional wideband radio signals in DM scenarios.

Besides using higher bandwidth, another way to increase the performance is to use multiple input, multiple output (MIMO) systems. For passive RFID tags the use of multiple antennas at the transmitter, tag and receiver have been analyzed with respect to the received power and bit error rate [9]–[12]. For ranging/positioning a MIMO-radar system can be employed using the geometric spread of the sensors and narrowband signals [13]. For classical outdoor radar applications the received signal consists of the backscattered LOS signal and additive white Gaussian noise (AWGN). Due to the previously introduced channel model the signal model for RFID radar systems operating indoors needs to be adapted leading to severe fading and distortions.

The main contributions of this paper are the following:

- We develop the ranging error variance for correlated and uncorrelated backscatter channels.
- We characterize the achievable ranging gain for multiple antennas in a monostatic setup.
- We discuss the position error bound for several readers leading to a MIMO RFID system.

The rest of this paper is organized as follows. Section II defines the system and signal model, which is used in Secton III to develop the ranging error variance for correlated and uncorrelated channels. Section IV re-visits the relation between the range and the position estimation errors and demonstrates how diversity combining can be expressed in terms of monostatic and bistatic accuracy gains. Section V draws conclusions and presents an outlook.

II. System and Channel Model

A. System Model

We consider L radio frequency identification (RFID) readers operating indoors at known positions $\mathbf{p}_\ell, \forall \ell \in \{1, \ldots, L\}$. Each reader consists of K closely-spaced antennas that can all be used to transmit and receive wideband signals (K TRX per reader). The signal $s(t)$ denotes the baseband equivalent transmit signal. The M RFID tags placed within the room at unknown positions $\mathbf{p}^{(m)}, \forall m \in \{1, \ldots, M\}$ scatter back the signal to the readers which in turn receive this signal. The according multiple input multiple output (MIMO) system model is depicted in Fig. 1.

This work was supported by the Austrian Research Promotion Agency (FFG) within the project "REFlex" (project number: 845630)

This paper has been published at the 2016 IEEE International Conference on RFID [1].

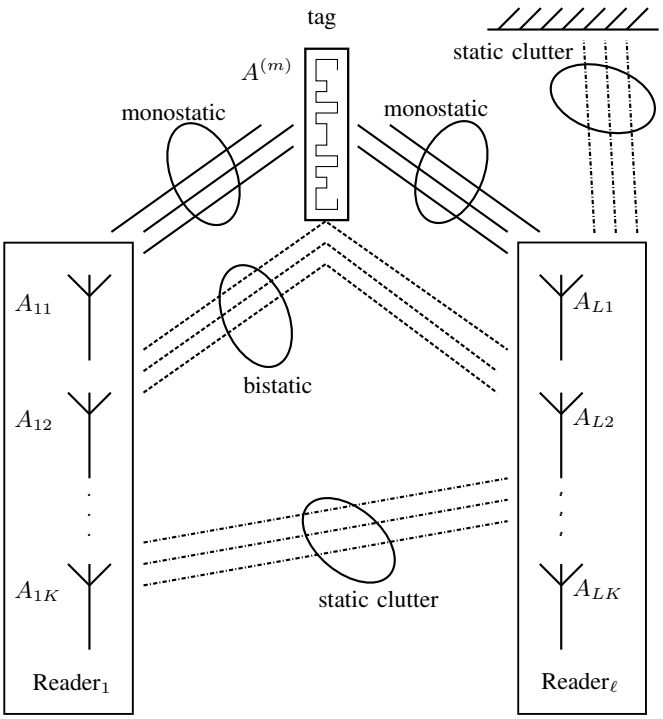

Fig. 1. System Model of the MIMO RFID setup including monostatic, bistatic and multistatic scenarios

The solid lines in Fig. 1 characterize monostatic links connecting antennas from reader ℓ via the tag with itself. Each monostatic link consists of two consituent channels, the downlink from one reader antenna $\mathrm{A}_{\ell k}$ to the tag antenna $\mathrm{A}^{(m)}$ and the uplink from the tag antenna $\mathrm{A}^{(m)}$ back to the same reader but not necessarily the same antenna $\mathrm{A}_{\ell k'}$. As we will see in Section II-C these channels can be modelled as correlated or uncorrelated.

The dashed lines in Fig. 1 represent bistatic links connecting antennas from two different readers, $\mathrm{A}_{\ell k}$ and $\mathrm{A}_{\ell' k'}$, via the tag antenna $\mathrm{A}^{(m)}$. Since the different readers are placed at different positions in the room, these channels will be modelled uncorrelated.

The dashed dotted lines in Fig. 1 depict static clutter that can be canceled from the received signal depending on the employed signaling scheme (cf. [4], [14], [15]).

B. Channel Model

Each individual baseband radio channel between any reader antenna $A_{\ell k}$ and a tag antenna $A^{(m)}$ is modeled by a hybrid deterministic-stochastic channel model [16]

$$h_{\ell k}^{(m)}(\tau) = \alpha_{\ell k}^{(m)} \delta(\tau - \tau_{\ell k}^{(m)}) + \nu_{\ell k}^{(m)}(\tau), \tag{1}$$

where $\alpha_{\ell k}^{(m)}$ describes the complex amplitude of the deterministic line-of-sight (LOS) component with delay $\tau_{\ell k}^{(m)} = \frac{1}{c}\|\mathbf{p}^{(m)} - \mathbf{p}_{\ell k}\|$, with c as the speed of light. The second term on the right hand side in (1) denotes the dense multipath (DM) which models all other multipath components. This DM is modeled as a zero-mean complex Gaussian random process. We assume uncorrelated scattering (US) [17], [18] along the delay axis τ for the DM process which means that the autocorrelation (ACF) of the DM is given as

$$\begin{aligned} K_\nu(\tau, u) &= \mathbb{E}\left\{\nu_{\ell k}^{(m)}(\tau)\nu_{\ell k}^{(m)}(u)^*\right\} \\ &= S_{\nu,\ell k}^{(m)}(\tau - \tau_{\ell k}^{(m)})\delta(\tau - u). \end{aligned} \tag{2}$$

The power delay profile (PDP) $S_{\nu,\ell k}^{(m)}(\tau - \tau_{\ell k}^{(m)})$ is zero for $\tau < \tau_{\ell k}^{(m)}$ implying that the DM does not exist until the LOS component excites the channel. We also assume quasi-stationarity in the spatial domain, meaning that for one reader-tag configuration, the PDP does not change noticeably in the vicinity of the tag [19].

The following derivation of the backscatter channel model does not restrict the usage to a certain model for the PDP; different choices for the PDP could be an exponentially decreasing PDP or a double exponential PDP [20]. For easier readability only one tag is considered in the following, thus the tag index m will be dropped. This does not limit the system model since various multiple access schemes can be employed to handle multiple tags and to separate the signals from different readers [4], [14], [15].

C. Backscatter Channel Model

One backscatter channel is formed by concatenation of the respective uplink channel $h_{\ell k}$ with a downlink channel $h_{\ell' k'}$. This pinhole channel can be modelled by the convolution of the two constituent channels as

$$\begin{aligned} h_{\ell k,\ell' k'} &= (h_{\ell k} * h_{\ell' k'})(\tau) \\ &= \alpha_{\ell k}\alpha_{\ell' k'}\delta(\tau - \tau_{\ell k} - \tau_{\ell' k'}) \\ &\quad + \alpha_{\ell k}\nu_{\ell' k'}(\tau - \tau_{\ell k}) + \alpha_{\ell' k'}\nu_{\ell k}(\tau - \tau_{\ell' k'}) \\ &\quad + \nu_{\ell k}(\tau) * \nu_{\ell' k'}(\tau). \end{aligned} \tag{3}$$

The first term in (3) shows the deterministic part of the backscatter channel. The second and third terms are the convolution of the DM of the downlink channel with the deterministic part of the uplink channel, and vice versa. Finally, the fourth term is the convolution of the two DM processes of the individual radio channels. By combining the last three terms in (3) to $\nu_{\ell k,\ell' k'}(\tau)$, the backscatter channel can be decomposed into a deterministic and a stochastic part resulting in a similar structure as for the individual channel in (1). The model in (3) assumes constant backscattering of the tag over the whole used bandwidth. This assumption does certainly not hold true for the UWB case, but the smaller the bandwidth gets, the less frequency dependent the radar cross section of a tag gets [21], [22].

Using the quasi-stationarity and the US assumption, the PDP of the backscatter channel is the second central moment of the DM process. Since the DM is described by a zero-mean Gaussian process, first and second moment give a complete description of the random process. In [23] the US assumption has been proven for a backscatter channel consisting of two US channels. Using $\nu_{\ell k,\ell' k'}(\tau)$ as the sum of the last three terms in (3), the PDP of the BS channel for two uncorrelated channels is [24]

$$S_{\nu,\ell k,\ell' k'}(\tau) = \mathbb{E}\left\{\nu_{\ell k,\ell' k'}(\tau)\nu_{\ell k,\ell' k'}^*(\tau)\right\} \tag{4}$$

$$
\begin{aligned}
&= |\alpha_{\ell k}|^2 S_{\nu,\ell' k'}(\tau - \tau_{\ell k}) \\
&\quad + |\alpha_{\ell' k'}|^2 S_{\nu,\ell k}(\tau - \tau_{\ell' k'}) \\
&\quad + S_{\nu,\ell k}(\tau) * S_{\nu,\ell' k'}(\tau).
\end{aligned}
$$

For two fully correlated constituent channels, e.g. the downlink and the uplink are the same, the PDP is [23]

$$
\begin{aligned}
S_{\nu,\ell k,\ell k}(\tau) &= \mathbb{E}\left\{\nu_{\ell k,\ell k}(\tau)\nu^*_{\ell k,\ell k}(\tau)\right\} \qquad (5)\\
&= 4|\alpha_{\ell k}|^2 S_{\nu,\ell k}(\tau - \tau_{\ell k}) + 2S_{\nu,\ell k}(\tau) * S_{\nu,\ell k}(\tau).
\end{aligned}
$$

The power in the non-line-of-sight (NLOS) components is thus twice as high for fully correlated channels as for uncorrelated constituent channels. In comparison the power in the LOS component is the same for correlated and uncorrelated constituent channels.

D. Received Signal

RFID reader ℓ transmits a baseband pulse $s(t)$ via anntena k and the downlink channel $h_{\ell k}(\tau)$ to the tag. Assuming perfect backscattering by the tag, the signal is then fed via the uplink channel $h_{\ell' k'}(\tau)$ and antenna k' to RFID reader ℓ'. The received signal is given as

$$
\begin{aligned}
r(t) &= s(t) * h_{\ell k,\ell' k'}(t) + \omega(t) \qquad (6)\\
&= \alpha_{\ell k}\alpha_{\ell' k'} s(t - \tau_{\ell k} - \tau_{\ell' k'}) + s(t) * \nu_{\ell k,\ell' k'}(t) + \omega(t),
\end{aligned}
$$

where $\omega(t)$ is additive white Gaussian noise (AWGN) with a two-sided power spectral density of $N_0/2$.

III. Ranging Error Bound and Performance Gain

In [8] we derived the ranging error bound for dense multipath channels which is the inverse of the square root of the equivalent Fisher information (EFI) for the delay estimation problem

$$
\mathcal{R}(\tau) = \sqrt{\mathcal{I}_\tau^{-1}}. \qquad (7)
$$

The EFI for an AWGN channel (neglecting multipath) is well known [25] and can be presented in a canonical form as

$$
\mathcal{I}^{\text{AWGN}}_{\tau,\ell k,\ell' k'} = 8\pi^2\beta^2 \text{SNR}_{\ell k,\ell' k'} \qquad (8)
$$

where $\beta^2 = \frac{\|\dot{\mathbf{s}}_\tau\|^2}{(4\pi^2\|\mathbf{s}_\tau\|^2} = \frac{\int_f f^2|S(f)|^2 \mathrm{d}f}{\int_f |S(f)|^2 \mathrm{d}f}$ is the effective (mean square) bandwidth of the (energy-normalized) transmit pulse $s(t) \overset{\mathcal{F}}{\longleftrightarrow} S(f)$, $\mathbf{s}_\tau$ is the sampled transmit pulse shifted to $\tau = \tau_{\ell k} + \tau_{\ell' k'}$, $\dot{\mathbf{s}}_\tau$ is its derivative, and $\text{SNR}_{\ell k,\ell' k'} = \frac{|\alpha_{\ell k}\alpha_{\ell' k'}|^2}{N_0}\|\mathbf{s}_\tau\|^2 T_s$ is the signal to noise ratio with $T_\text{s} = 1/f_\text{s}$, f_s being the sampling frequency.

Adding the Gaussian DM, the EFI can be presented for a single backscatter channel in a canonical form as [5]

$$
\begin{aligned}
\mathcal{I}_{\tau,\ell k,\ell' k'} &= 8\pi^2\beta^2\gamma \text{SINR}_{\ell k,\ell' k'} \qquad (9)\\
&= 8\pi^2\beta^2 \widetilde{\text{SINR}}_{\ell k,\ell' k'}, \qquad (10)
\end{aligned}
$$

where SINR is the signal-to-interference-plus-noise ratio (SINR) of the LOS component, and γ is the so-called whitening gain. The product of β^2, SINR, and γ thus provides the amount of information transmitted in the LOS component when influenced by DM and AWGN. For the derivation of (9), the inverse of the covariance matrix of DM plus AWGN is needed as a whitening operator. The SINR and the whitening gain γ are also combined in the effective SINR, $\widetilde{\text{SINR}}$ which can be expressed as (see the appendix)

$$
\widetilde{\text{SINR}}_{\ell k,\ell' k'} = \frac{|\alpha_{\ell k}\alpha_{\ell' k'}|^2}{N_0}\|\mathbf{s}_\tau\|^2 T_s \frac{\|\dot{\mathbf{s}}_\tau\|^2_{\mathcal{H}}}{\|\dot{\mathbf{s}}_\tau\|^2}\sin^2(\phi), \qquad (11)
$$

where $\|\cdot\|^2_{\mathcal{H}}$ denotes the weighted squared norm in a Hilbert space defined by the covariance $\mathbf{C}_\text{n}/\sigma^2_\text{n}$ (see the appendix), and ϕ is the angle between $\mathbf{s}_\tau$ and its derivative $\dot{\mathbf{s}}_\tau$ in this Hilbert space.

In Fig. 2 the SINR, $\widetilde{\text{SINR}}$, and γ are shown for a monostatic setup for fully correlated and for uncorrelated constituent channels with solid and dashed lines respectively over a wide range of bandwidths (BW). The necessary distance between the downlink and uplink of the backscatter channel to be (at least partially) uncorrelated is characterized by the correlation distance which is defined as the distance at which the correlation of two channel impulse responses drops below a given value (e.g. 50 %). For uniformly distributed angle-of-arrivals the correlation distance is in the order of the wavelength λ [26]. The SINR is bound for high BW by the signal to noise ratio (SNR) and for low BW by the Rician K-factor of the backscatter channel.[1] For high bandwidths the effective SINR is also bound by the SNR, while for low bandwidths the $\widetilde{\text{SINR}}$ achieves the SNR as well. The effective SINR is in fact a measure of the pulse distortion rather than the fading of the LOS component [8].

The REB decreases linearly with the effective bandwidth in conformity with (10). According to Fig. 2 the effective SINR increases from about 10 MHz also with increasing bandwidth; thus the REB decreases slightly more than linearly with the bandwidth.

The gain in SINR achieved by using two closely-spaced antennas with uncorrelated constituent channels in a monostatic setup is 3 dB for low BW and gets 0 dB for high BW, where the whitening gain is already negligible, since the LOS component is isolated from the DM and the channel is AWGN dominated. The gain for $\widetilde{\text{SINR}}$ is highest in the medium BW region where the most pulse disortion occurs and is about 2 dB. This gain for SINR and $\widetilde{\text{SINR}}$ for uncorrelated channels is explained by the additional power in the DM process according to Section II-C.

Looking at a 1-dimensional positioning scenario, e.g. positioning on a conveyor belt, where only ranging is needed, the EFI from (10) can be extended for one RFID reader with K antennas as

$$
\mathcal{I}_{\tau,\ell K} = 8\pi^2\beta^2 \sum_{k=1}^{K}\sum_{k'=k}^{K} \widetilde{\text{SINR}}_{\ell k,\ell k'}. \qquad (12)
$$

This equation holds for antenna arrays which are closely spaced with respect to the distance between the tag and the center point of the array. The second sum in (12) only indexes $K{-}k{+}1$ terms, since the channel from k to k' and the reverse

[1] For Fig. 2 the K_LOS factor for the constituent channels are chosen such that the backscatter channel has an overall K_LOS of 1 [23].

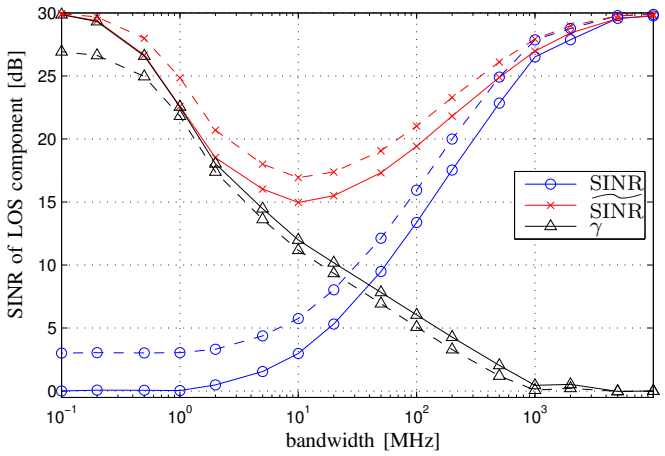

Fig. 2. SINR, $\widetilde{\text{SINR}}$, and whitening gain γ for a monostatic setup with correlated (solid line) and uncorrelated (dashed line) constituent channels. Constituent Channel Parameters: $K_{\text{LOS}} = 6.4\,\text{dB}$, $\gamma_{\text{rise}} = 5\,\text{ns}$, $\gamma_{\text{dec}} = 20\,\text{ns}$, $E_{\text{LOS}}/N_0 = 30\,\text{dB}$

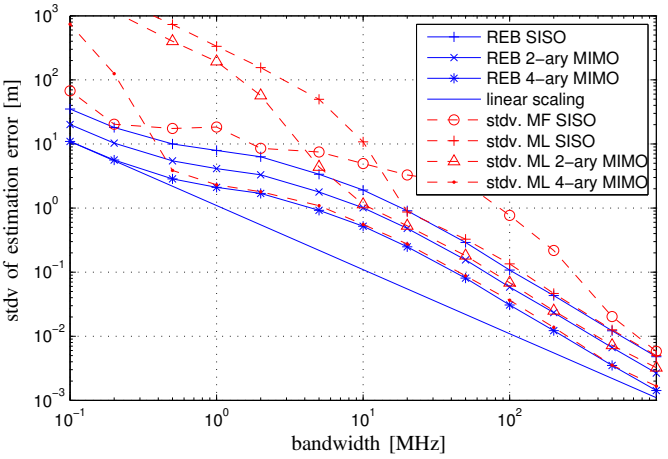

Fig. 3. Ranging Error Bound for monostatic setup, 2-Array reader, 4-Array reader and standard deviations for different estimators. Constituent Channel Parameters: $K_{\text{LOS}} = 6.4\,\text{dB}$, $\gamma_{\text{rise}} = 5\,\text{ns}$, $\gamma_{\text{dec}} = 20\,\text{ns}$, $E_{\text{LOS}}/N_0 = 30\,\text{dB}$

channel from k' to k are the same (reciprocity) thus no new observation of the DM process is obtained.

For an antenna array with K antennas, K fully correlated and $\sum_{k=1}^{K-1} k = \frac{K(K-1)}{2}$ uncorrelated backscatter channels are available, leading to a total effective SINR of

$$\begin{aligned}\widetilde{\text{SINR}}_{\text{total}} &= K\widetilde{\text{SINR}}_{\ell k,\ell k} + \frac{K(K-1)}{2}\widetilde{\text{SINR}}_{\ell k,\ell k'} \\ &= \left(K + g_{\text{uncorr}}\frac{K(K-1)}{2}\right)\widetilde{\text{SINR}}_{\ell k,\ell k} \\ &\approx K^2\widetilde{\text{SINR}}_{\ell k,\ell k},\end{aligned} \tag{13}$$

where g_{uncorr} is the gain in $\widetilde{\text{SINR}}$ for an uncorrelated versus a correlated measurement and is approximated as 2 for the final approximation.

In Fig. 3 the REB is depicted for different reader arrays. The gain due to the twofold antenna array and 4-ary antenna array is shown by the REB. From (12) and Fig. 3 it is clear that the REB scales slightly more than linearly with the bandwidth. According to (13) the number of antennas also scales the REB linearly. However, the gain for using uncorrelated constituent channels is smaller than 2, thus the gain for using additional antennas is smaller than for increasing the bandwidth.

By simulating a ranging scenario with one RFID reader with K antennas the REB can be evaluated. For the following simulations, a double exponential PDP is used to model the NLOS contributions by the DM process [20]. For ranging two different estimators are used, a classical matched filter (MF) and a maximum likelihood (ML) estimator. The accuracy gain due to the whitening operation used for the ML estimator is especially noticeable for BW between 50 and 500 MHz. The better performance of the MF estimator at low BW can be explained by the fact, that the complete DM interferes with the LOS, thus the MF uses the power in the DM also for ranging. The ML estimator, in contrast, will suppress the DM process due to the whitening filter.

The accuracy gain for the K-ary array is also shown by the standard deviations of the estimator errors. Furthermore, a detection gain can be identified when inspecting the curves for the ML estimator for SISO and MIMO processing. The ML estimator achieves the REB at lower bandwidths since the detection of the LOS is enhanced, similarily as the bit error rate is decreased for MIMO processing in communication systems. While the detection gain is impressive at bandwidth below 10 MHz the limit for useable indoor positioning, assuming a ranging accuracy in the submeter range, is roughly in the range from 20 to 100 MHz.

IV. Positioning Error Bound and Performance Gain

The position error bound (PEB) is the square root of the trace of the inverse EFI matrix (EFIM) on the position estimation error

$$\mathcal{P}\{\mathbf{p}\} = \sqrt{\text{tr}\{\boldsymbol{\mathcal{I}}_{\mathbf{p}}^{-1}\}} \leq \sqrt{\mathbb{E}\left\{\|\mathbf{p}-\hat{\mathbf{p}}\|^2\right\}} \tag{14}$$

and can be computed from the EFI for the delay estimation with the chain rule as [5], [6]

$$\begin{aligned}\boldsymbol{\mathcal{I}}_{\mathbf{p}} = &\sum_{\ell=1}^{L}\sum_{k=1}^{K}\sum_{k'=k}^{K}\mathcal{I}_{\tau,\ell k,\ell k'}\mathbf{h}_{\ell k,\ell k'}\mathbf{h}_{\ell k,\ell k'}^{\mathbf{T}} \\ &+\sum_{\ell=1}^{L-1}\sum_{\ell'=\ell+1}^{L}\sum_{k=1}^{K}\sum_{k'=1}^{K}\mathcal{I}_{\tau,\ell k,\ell' k'}\mathbf{h}_{\ell k,\ell' k'}\mathbf{h}_{\ell k,\ell' k'}^{\mathbf{T}},\end{aligned} \tag{15}$$

where the first term accounts for the monostatic channels between an RFID reader with itself, and the second term relates to the bistatic channels between two different readers leading to a multistatic scenario (cf. Fig. 1). The geometry of the setup is expressed by $\mathbf{h}_{\ell k,\ell' k'}$ as (cf. [5], [6], [13])

$$\mathbf{h}_{\ell k,\ell' k'}^{(m)} = \frac{1}{c}(\mathbf{e}_{\ell k}^{(m)} + \mathbf{e}_{\ell' k'}^{(m)}), \tag{16}$$

where we included the index of the tag for completeness and $\mathbf{e}_{\ell k}^{(m)}$ is a unit vector in the direction between the m-th tag and the k-th antenna of the ℓ-th reader. Using the

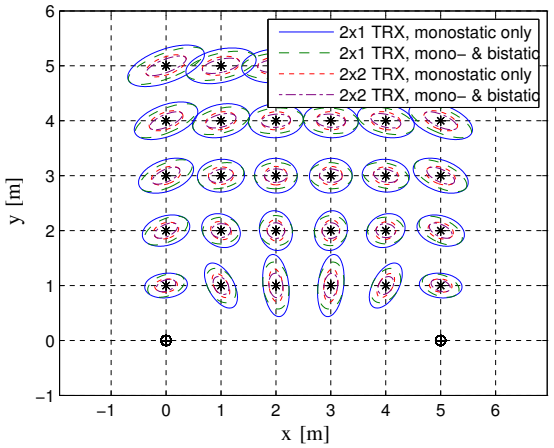

Fig. 4. 2-fold standard deviation ellipses for a bandwidth of 50 MHz and different MIMO constellations. Constituent Channel Parameters: distance dependent K_{LOS} [23], $\gamma_{\mathrm{rise}} = 5\,\mathrm{ns}$, $\gamma_{\mathrm{dec}} = 20\,\mathrm{ns}$, $E_{\mathrm{LOS}}/N_0 = 30\,\mathrm{dB}$

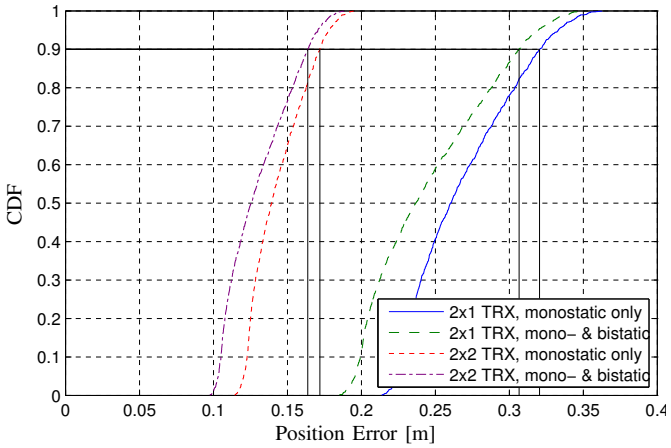

Fig. 5. Cumulative Distribution Function of the Position Error Bound for a bandwidth of 50 MHz for a 10 cm spacing in a half plane and different MIMO constellations. Constituent Channel Parameters: distance dependent K_{LOS} [23], $\gamma_{\mathrm{rise}} = 5\,\mathrm{ns}$, $\gamma_{\mathrm{dec}} = 20\,\mathrm{ns}$, $E_{\mathrm{LOS}}/N_0 = 30\,\mathrm{dB}$

approximation that for closely spaced antennas the unit vector $\mathbf{e}_{\ell k}^{(m)} \approx \mathbf{e}_{\ell k'}^{(m)}, \forall k, k'$ and introducing $\mathbf{h}_{\ell,\ell'}$ for $\mathbf{h}_{\ell k,\ell' k'}^{(m)}$, (15) can be written with (13) as

$$\begin{aligned}\boldsymbol{\mathcal{I}}_{\mathbf{p}} \approx\ & 8\pi^2\beta^2 K^2 \sum_{\ell=1}^{L} \widetilde{\mathrm{SINR}}_{\ell,\ell}\mathbf{h}_{\ell,\ell}\mathbf{h}_{\ell,\ell}^{\mathbf{T}} \\ & + 8\pi^2\beta^2 K^2 \sum_{\ell=1}^{L-1}\sum_{\ell'=\ell+1}^{L} \widetilde{\mathrm{SINR}}_{\ell,\ell'}\mathbf{h}_{\ell,\ell'}\mathbf{h}_{\ell,\ell'}^{\mathbf{T}}.\end{aligned} \tag{17}$$

By increasing the number of antennas per reader, the EFIM for the position error scales with the square of the number of antennas K in both the monostatic directions and the bistatic directions. Thus the PEB decreases linearly with respect to the number of antennas in the directions defined by $\mathbf{h}_{\ell,\ell}^{(m)}$ and $\mathbf{h}_{\ell,\ell'}^{(m)}$. Furthermore, by increasing the number of readers, the gain in monostatic directions is achieved L-times, while the gain in bistatic directions is applied $\frac{L(L-1)}{2}$-times.

In Fig. 4 the 2-fold standard deviation ellipses are depicted for different tag positions in a half plane. These ellipses can be computed from the inverse of the position EFIM $\boldsymbol{\mathcal{I}}_{\mathbf{p}}$. One RFID reader is positioned at $[0\ 0]^{\mathbf{T}}$ and another reader at $[5\ 0]^{\mathbf{T}}$. These readers are either equipped with one or two TRX, dependening on the scenario. The first two scenarios (2x1TRX monostatic only, and 2x1TRX mono- and bistatic) use one TRX, while the latter two scenarios (2x2TRX monostatic only, and 2x2TRX mono- and bistatic) use two TRX at each reader. For the first and third scenario, no time synchronisation is needed between the RFID readers, since only backscatter channels are used that originate and end at the same reader.

Within these scenarios, the influence of the geometry is clearly visible. According to (16) monostatic measurements (Scenarios 1 and 3) add information only in the radial directions, corresponding to circles around the readers. Bistatic measurements (between two different readers) add information mainly in the orthogonal axis, which corresponds to the normal direction of an ellipse with the two readers in its foci. In Fig. 4 this directional information gain is well visible since the ellipses for the mono- and bistatic scenarios are tangent to the monostatic scenarios in one direction, while an information gain is seen for the orthogonal direction.

By comparing the ellipses for Scenarios 1 and 2 with the Scenarios 3 and 4, respectively, the accuracy gain for additional antennas can be seen. The ellipses for Scenarios 3 and 4 have the same orientations as for Scenarios 1 and 2, and are K-times smaller.

To evaluate the overall potential positioning performance in the half plane, the PEB is displayed in Fig. 5 for a 10 cm spacing over the half plane. The gain by adding an additional antenna is about a factor of two like described by (17).

V. Conclusions and Outlook

The MIMO gain and bandwidth scaling have been analyzed for RFID positioning in dense multipath scenarios. The error standard deviation for additional antennas scales roughly linearly with respect to a single monostatic link. Increasing the bandwidth scales the standard deviation of each measurement slightly more than linearly, leading to a higher gain. Furthermore, additional antennas also show a detection gain enabling the usage of lower bandwidths. The next steps are to validate these findings by measurements and develop algorithms which are able to employ the theoretical findings. 1

Appendix

The EFI is defined as the second moment of the partial derivative of the log-likelihood function [25]. By sampling the received signal in (6) the likelihood function conditioned on the parameter vector $\boldsymbol{\psi} = [\tau, \Re\alpha, \Im\alpha]$ is defined as

$$f(\mathbf{r}|\boldsymbol{\psi}) \propto \exp\left\{-(\mathbf{r} - \mathbf{s}_\tau\alpha)^{\mathrm{H}}\mathbf{C}_{\mathrm{n}}^{-1}(\mathbf{r} - \mathbf{s}_\tau\alpha)\right\} \tag{A.18}$$

where the covariance matrix of DM and AWGN is

$$\mathbf{C}_{\mathrm{n}} = \sigma_{\mathrm{n}}^2\mathbf{I}_N + \mathbf{C}_{\mathrm{c}} = \sigma_{\mathrm{n}}^2\mathbf{I}_N + \bar{\mathbf{S}}^{\mathrm{H}}\mathbf{S}_{\nu,\ell k,\ell' k'}\bar{\mathbf{S}}, \tag{A.19}$$

where $\bar{\mathbf{S}} = [\mathbf{s}_0, \cdots, \mathbf{s}_{N-1}]^{\mathrm{T}} \in \mathbb{R}^{N\times N}$ is the *full* signal matrix with $\mathbf{s}_i = \Big[s((-i)T_{\mathrm{s}}), \ldots, s((N-1-i)T_{\mathrm{s}})\Big]^{\mathrm{T}}$ [5]. The elements of the covariance matrix are

$$[\bar{\mathbf{S}}^{\mathrm{H}}\mathbf{S}_{\nu\ell k,\ell' k'}\bar{\mathbf{S}}]_{n,m} = \sum_{i=0}^{N-1} T_{\mathrm{s}} S_{\nu\ell k,\ell' k'}(iT_{\mathrm{s}}) \times s((n-i)T_s)s((m-i)T_s). \tag{A.20}$$

The derivation of the FIM under non-stationary, non-white Gaussian noise, involves a whitening operation that is defined by the inverse of the covariance matrix. By utilizing an eigenvector decomposition for the covariance matrix, we introduce the Fourier weighted inner product in a Hilbert space defined [8] by

$$\begin{aligned}\frac{\langle \mathbf{x}, \mathbf{y}\rangle_{\mathcal{H}}}{\sigma_{\mathrm{n}}^2} &= \mathbf{y}^{\mathbf{H}}\mathbf{C}_n^{-1}\mathbf{x} \\ &= \mathbf{y}^{\mathbf{H}}\mathbf{U}(\mathbf{\Lambda} + \sigma_{\mathrm{n}}^2\mathbf{I}_N)^{-1}\mathbf{U}^{\mathrm{H}}\mathbf{x} \\ &= \frac{1}{\sigma_{\mathrm{n}}^2}\sum_{i=0}^{N-1}\frac{\mathbf{y}^{\mathrm{H}}\mathbf{u}_i\mathbf{u}_i^{\mathrm{H}}\mathbf{x}}{\lambda_i/\sigma_{\mathrm{n}}^2+1}\end{aligned} \tag{A.21}$$

to completely define the FIM. This yields the SINR of the LOS component as

$$\mathrm{SINR}_{\ell k\ell' k'} = \frac{|\alpha_{\ell k}\alpha_{\ell' k'}|^2}{N_0}\|\mathbf{s}_\tau\|_{\mathcal{H}}^2 T_s \sin^2(\phi), \tag{A.22}$$

where $\|\cdot\|_{\mathcal{H}}^2$ denotes the squared norm in the Hilbert space, and ϕ is the angle between $\mathbf{s}_\tau$ and its derivative $\dot{\mathbf{s}}_\tau$ in this Hilbert space. It can cleary be seen, that the SINR is directly influenced by the power of the DM which is reflected in the eigenvalues λ_i in the whitening operation. The whitening gain is

$$\gamma = \frac{\|\dot{\mathbf{s}}_\tau\|_{\mathcal{H}}^2\|\mathbf{s}_\tau\|^2}{\|\dot{\mathbf{s}}_\tau\|^2\|\mathbf{s}_\tau\|_{\mathcal{H}}^2}, \tag{A.23}$$

and the effective SINR is

$$\widetilde{\mathrm{SINR}}_{\ell k\ell' k'} = \frac{|\alpha_{\ell k}\alpha_{\ell' k'}|^2}{N_0}\|\mathbf{s}_\tau\|^2 T_s \frac{\|\dot{\mathbf{s}}_\tau\|_{\mathcal{H}}^2}{\|\dot{\mathbf{s}}_\tau\|^2}\sin^2(\phi). \tag{A.24}$$

REFERENCES

[1] S. Hinteregger, E. Leitinger, P. Meissner, and K. Witrisal, "MIMO gain and bandwidth scaling for RFID positioning in dense multipath channels," in *2016 IEEE International Conference on RFID (RFID)*, May 2016, pp. 1–6.

[2] G. Li, D. Arnitz, R. Ebelt, U. Muehlmann, K. Witrisal, and M. Vossiek, "Bandwidth dependence of CW ranging to UHF RFID tags in severe multipath environments," in *2011 IEEE International Conference on RFID (RFID)*, April 2011, pp. 19–25.

[3] D. Dardari, A. Conti, U. Ferner, A. Giorgetti, and M. Z. Win, "Ranging with ultrawide bandwidth signals in multipath environments," *Proc. IEEE*, vol. 97, no. 2, pp. 404–426, 2009.

[4] H. Arthaber, T. Faseth, and F. Galler, "Spread-spectrum based ranging of passive UHF EPC RFID tags," *IEEE Commun. Lett.*, vol. 19, no. 10, pp. 1734–1737, Oct 2015.

[5] E. Leitinger, P. Meissner, C. Rudisser, G. Dumphart, and K. Witrisal, "Evaluation of position-related information in multipath components for indoor positioning," *IEEE J. Sel. Areas Commun.*, vol. 33, no. 11, pp. 2313–2328, Nov 2015.

[6] Y. Shen and M. Z. Win, "Fundamental limits of wideband localizationpart i: A general framework," *IEEE Trans. Inf. Theory*, vol. 56, no. 10, pp. 4956–4980, 2010.

[7] A. Richter and R. S. Thoma, "Joint maximum likelihood estimation of specular paths and distributed diffuse scattering," in *IEEE Vehicular Technology Conference, VTC 2005-Spring*, 2005.

[8] K. Witrisal, E. Leitinger, S. Hinteregger, and P. Meissner, "Bandwidth scaling and diversity gain for ranging and positioning in dense multipath channels," *IEEE Wireless Communications Letters*, 2016.

[9] M. A. Ingram, M. F. Demirkol, and D. Kim, "Transmit diversity and spatial multiplexing for RF links using modulated backscatter," in *Proceedings of the International Symposium on Signals, Systems and Electronics, Tokyo*, July, 2001.

[10] J. D. Griffin and G. D. Durgin, "Gains for RF tags using multiple antennas," *IEEE Trans. Antennas Propag.*, vol. 56, no. 2, pp. 563–570, Feb 2008.

[11] ——, "Multipath fading measurements for multi-antenna backscatter RFID at 5.8 GHz," in *2009 IEEE International Conference on RFID*, April 2009, pp. 322–329.

[12] C. He, X. Chen, Z. J. Wang, and W. Su, "On the performance of MIMO RFID backscattering channels," *EURASIP Journal on Wireless Communications and Networking*, vol. 2012, no. 1, p. 115, 2012.

[13] H. Godrich, A. M. Haimovich, and R. S. Blum, "Target localization accuracy gain in MIMO radar-based systems," *IEEE Trans. Inf. Theory*, vol. 56, no. 6, pp. 2783–2803, June 2010.

[14] D. Dardari, R. D'Errico, C. Roblin, A. Sibille, and M. Z. Win, "Ultrawide bandwidth RFID: The next generation?" *Proc. IEEE*, vol. 98, no. 9, pp. 1570–1582, Sept 2010.

[15] D. Arnitz, U. Muehlmann, and K. Witrisal, "UWB ranging in passive UHF RFID: Proof of concept," *Electronics Letters*, vol. 46, no. 20, pp. 1401–1402, September 2010.

[16] K. Witrisal and P. Meissner, "Performance bounds for multipath-assisted indoor navigation and tracking (MINT)," in *IEEE International Conference on Communications (ICC)*, 2012.

[17] P. Bello, "Characterization of randomly time-variant linear channels," *IEEE Transactions on Commun. Sys.*, vol. 11, no. 4, pp. 360 –393, december 1963.

[18] A. F. Molisch, *Wireless Communications*. Wiley-IEEE Press, 2005.

[19] ——, "Ultra-wide-band propagation channels," *Proc. IEEE*, vol. 97, no. 2, pp. 353–371, Feb 2009.

[20] J. Karedal, S. Wyne, P. Almers, F. Tufvesson, and A. F. Molisch, "A measurement-based statistical model for industrial ultra-wideband channels," *IEEE Trans. Wireless Commun.*, vol. 6, no. 8, pp. 3028–3037, August 2007.

[21] P. V. Nikitin and K. V. S. Rao, "Theory and measurement of backscattering from RFID tags," *IEEE Antennas Propag. Mag.*, vol. 48, no. 6, pp. 212–218, Dec 2006.

[22] D. Arnitz, U. Muehlmann, and K. Witrisal, "Tag-based sensing and positioning in passive UHF RFID: Tag reflection," in *3rd Int EURASIP workshop on RFID Technology*, 2010.

[23] ——, "Wideband characterization of backscatter channels: Derivations and theoretical background," *IEEE Trans. Antennas Propag.*, vol. 60, no. 1, pp. 257–266, Jan 2012.

[24] E. Leitinger, P. Meissner, M. Frohle, and K. Witrisal, "Performance bounds for multipath-assisted indoor localization on backscatter channels," in *2014 IEEE Radar Conference*, May 2014, pp. 0070–0075.

[25] S. Kay, *Fundamentals of Statistical Signal Processing: Estimation Theory*. Prentice Hall Signal Processing Series, 1993.

[26] D. Arnitz, U. Muehlmann, and K. Witrisal, "Characterization and modeling of UHF RFID channels for ranging and localization," *IEEE Trans. Antennas Propag.*, vol. 60, no. 5, pp. 2491–2501, May 2012.